Elsevier Editorial System(tm) for International Journal of Applied Earth Observation and Geoinformation

Manuscript Draft

Manuscript Number: JAG-D-12-00182R1

Title: Optical and SAR sensor synergies for forest and land cover mapping in a tropical site in West Africa

Article Type: Research Paper

Keywords: Classification; West Africa; Forests; SAR; Landsat; AVNIR-2; Texture

Corresponding Author: Mrs Gaia Vaglio Laurin,

Corresponding Author's Institution:

First Author: Gaia Vaglio Laurin

Order of Authors: Gaia Vaglio Laurin; Veraldo Liesenberg; Qi Chen; Leila Guerriero; Fabio Del Frate; Antonio Bartolini; David Coomes; Beccy Wilebore; Jeremy Lindsell; Riccardo Valentini

Abstract: Abstract: The classification of tropical fragmented landscapes and moist forested areas is a challenge due to the presence of a continuum of vegetation successional stages, persistent cloud cover and the presence of small patches of different land cover types. To classify one such study area in West Africa we integrated the optical sensors Landsat Thematic Mapper (TM) and the Advanced Visible and Near Infrared Radiometer type 2 (AVNIR-2) with the Phased Arrayed L-band SAR (PALSAR) sensor, the latter two on-board the Advanced Land Observation Satellite (ALOS), using traditional Maximum Likelihood (MLC) and Neural Networks (NN) classifiers. The impact of texture variables and the use of SAR to cope with optical data unavailability were also investigated. SAR and optical integrated data produced the best classification overall accuracies using both MLC and NN, respectively equal to 91.1% and 92.7% for TM and 95.6% and 97.5% for AVNIR-2. Texture information derived from optical images was critical, improving results between 10.1 % and 13.2%. In our study area, PALSAR alone was able to provide valuable information over the entire area: when the three forest classes were aggregated, it achieved 75.7% (with MCL) and 78.1% (with NN) overall classification accuracies. The selected classification and processing methods resulted in fine and accurate vegetation mapping in a previously untested region, exploiting all available sensors synergies and highlighting the advantages of each dataset.

This is an accepted manuscript of an article published by Elsevier in the International Journal of Applied Earth Observation and Geoinformation on 15 September 2012, available online: https://doi.org/10.1016/j.jag.2012.08.002.

Optical and SAR sensor synergies for forest and land cover mapping in a tropical site in West Africa

Gaia Vaglio Laurin[a,g]*, Veraldo Liesenberg[b], Qi Chen[d], Leila Guerriero[a], Fabio Del Frate[a], Antonio Bartolini[a], David Coomes[c], Beccy Wilebore[c], Jeremy Lindsell[e], Riccardo Valentini[f,g].

[a]Tor Vergata University, Dipartimento di Informatica, Sistemi e Produzione, Via del Politecnico 1, 00133 Rome, Italy

[b]Remote Sensing Group, Institute for Geology, TU-Bergakademie Freiberg, Bernhard von Cotta Str. 2, 09599 Freiberg, Germany

[c]Forest Ecology and Conservation Group, Department of Plant Sciences, University of Cambridge, Downing Street, Cambridge CB2 3EA, UK.

[d]Department of Geography, University of Hawai`i at Mānoa, 422 Saunders Hall, 2424 Maile Way, Honolulu, HI, 96822, USA

[e]The Royal Society for the Protection of Birds, The Lodge, Sandy, Beds. SG19 2DL, UK.

[f]Department of Forest Resources and Environment, University of Tuscia, Viterbo I-01100 Italy

[g]CMCC - Centro Mediterraneo per i Cambiamenti Climatici, via Augusto Imperatore (Euro-Mediterranean Center for Climate Change), Lecce 73100, Italy

*Corresponding author: Email: laurin@disp.uniroma2.it; Phone/Fax: 0039 06 72597710

Optical and SAR sensor synergies for forest and land cover mapping in a tropical site in West Africa

Abstract: The classification of tropical fragmented landscapes and moist forested areas is a challenge due to the presence of a continuum of vegetation successional stages, persistent cloud cover and the presence of small patches of different land cover types. To classify one such study area in West Africa we integrated the optical sensors Landsat Thematic Mapper (TM) and the Advanced Visible and Near Infrared Radiometer type 2 (AVNIR-2) with the Phased Arrayed L-band SAR (PALSAR) sensor, the latter two on-board the Advanced Land Observation Satellite (ALOS), using traditional Maximum Likelihood (MLC) and Neural Networks (NN) classifiers. The impact of texture variables and the use of SAR to cope with optical data unavailability were also investigated. SAR and optical integrated data produced the best classification overall accuracies using both MLC and NN, respectively equal to 91.1% and 92.7% for TM and 95.6% and 97.5% for AVNIR-2. Texture information derived from optical images was critical, improving results between 10.1 % and 13.2%. In our study area, PALSAR alone was able to provide valuable information over the entire area: when the three forest classes were aggregated, it achieved 75.7% (with MCL) and 78.1% (with NN) overall classification accuracies. The selected classification and processing methods resulted in fine and accurate vegetation mapping in a previously untested region,

exploiting all available sensors synergies and highlighting the advantages of each dataset.

Keywords: Classification; West Africa; Forests; SAR; Landsat; AVNIR-2; Texture

1. Introduction

The classification of moist tropical areas is a challenging task for a number of reasons. Firstly, the atmospheric conditions cause persistent cloud cover and limit the use of optical data. Secondly, the landscape is often fragmented into small patches of different land use and land cover types. Furthermore, the peculiar characteristics of natural vegetation cause a continuous transition among vegetation types, making it difficult to spectrally differentiate various successional stages, as exemplified by Lu et al. (2007) over Amazonian moist forested regions.

The Upper Guinean forests of West Africa have experienced a dramatic decrease of their original extent. Logging, mining, hunting and human population growth are still placing extreme stress on this biodiversity hotspot (CEPF 2003). The few classification studies available for West Africa report problems in mapping forest and vegetation classes (Igue et al. 2006; Judex et al. 2006). Nevertheless, mapping activities are extremely important for conservation and planning issues and with respect to the emerging REDD+ (Reducing Emissions from Deforestation and Forest Degradation in Developing Countries) program (Gibbs et al., 2007). Detailed mapping is also important for national planning in many tropical countries, where local communities rely on woody vegetation as a primary source of products and energy (Avitabile et al. 2012).

Optical sensors have been the primary data sources for land cover classification since the launch of the Landsat satellite series in early 1970s. In recent years, Synthetic Aperture Radar (SAR) sensors have emerged as important tools for vegetation studies, being well suited to detect volumetric scattering, especially at L- and P- bands (Rahman and Sumantyo, 2010; Santos et al., 2004; Simard et al., 2000). Since radar can penetrate clouds, it is a supplementary data source when atmospheric conditions hamper optical data use (Lehmann et al., 2012; Lu et al., 2007, Mitchard et al., 2012). In general, the combination of the two data types is considered beneficial (Lefsky and Cohen 2003) because optical data allows the measurement of the reflectance of the topmost layer of the canopy and SAR data deliver useful geometric information without being affected by weather conditions. However, the benefits of data integration can vary according to landscape and specific sensors characteristics, making it useful to explore the synergistic use of different datasets in the West African region where, according to our knowledge, no classification study exists at a fine scale.

In addition to reflectance or backscattering coefficient, texture (the spatial arrangement of color or intensities of pixels) has been proved useful to improve classification accuracy (Berberoglu et al., 2007; Chica-Olmo & Abarca-Hernandez, 2000; Dekker, 2003; Dorigo et al., 2012; Lu et al., 2007). Textural differences can potentially be observed in optical data between the uneven canopy ‘topography’ of secondary and mixed semi-deciduous forests and the more uniform mature

evergreen forests, classes which are usually hard to distinguish. In fact, forests of different ages and types are known to structural differences, i.e. in canopy gaps and/or in tree height composition (Yavitt et al., 1995), resulting in shadows and different reflectance values that influence the texture variables calculated over near infrared (NIR) or short wave infrared highly reflecting bands. In the case of semi-deciduous forest, bare trees are seen at these wavelengths as low reflecting objects and therefore produce less smooth textures. It is known that shadows are a function of canopy structure and cover and Asner (1998) reports that both red and NIR wavelength regions are highly sensitive to sub-pixel shadow fractions in Amazon tropical forests. A number of studies have used texture from multiple remotely sensed data such as Landsat and Advanced Land Observation Satellite (ALOS) Phased Arrayed L-band SAR (PALSAR;1.27 GHz center frequency, 23 cm wavelength) for mapping tropical environments (Erasmi and Twelle, 2009; Kuplich, 2006; Longepe et al., 2011, Wijaya et al. 2008). For instance, Chan et al. (2003) used textures from Landsat data and machine learning techniques to improve discrimination of logged versus non-logged semi-deciduous forest classes in Central Africa. In Gabon, Simard et al. (2000) used texture from Japanese Earth Resources Satellite (JERS-1) SAR data to refine the classification of the flooded forest class. The permutation of different bands, window sizes, and texture variables could potentially generate a large number of texture features: given a training dataset of a certain size, including too many variables may decrease classification accuracy and a feature selection method can be beneficial (Price et al.

2003). In our research, a relatively simple and automatic wrapper based approach for feature selection is proposed, which is considered optimal for supervised learning problems (Talavera, 2005).

In this study, we primarily investigate the potential of combining optical and radar sensors for discriminating land cover classes for a moist tropical area which has never been classified by high resolution remote sensing before. The optical sensors to be tested are Landsat TM (Thematic Mapper) and ALOS AVNIR-2 (Advanced Visible and Near Infrared Radiometer type 2); the SAR sensor used is the dual polarimetric ALOS PALSAR. The specific research objectives are multifold: 1) to assess the results obtained by sensor integration; 2) to explore the degree SAR can support land cover and vegetation mapping when atmospheric conditions affect optical data availability and quality, 3) to assess the value of textures for improving vegetation classification.

2. Materials and methods

2.1 Study area

The study area (covering a total of 7749 km^2) spans the border of Sierra Leone and Liberia and includes the recently established Gola Rainforest National Park (GRNP) which is composed of three disjunct areas covering about 710 km^2 (North, Central and South), and most of the Liberian Gola National Forest (about 2300 km^2). In the north-west of the study area there is a fragmented landscape

comprising small patches of disturbed forest, farmbushes, plantations, active agriculture areas, bare lands and settlements; in the south-east the landscape is dominated by forests (Fig.1). Forests of the region are classified mainly as lowland moist evergreen with some drier parts occurrence, are dominated by *Fabaceae*, *Euphorbiaceae* and *Sterculiaceae* families (Cole, 1993).

Within Sierra Leone, the protected areas comprise the GRNP and Tiwai Island Wildlife Sanctuary. Inside GRNP, recent field surveys (Klop et al., 2008) identified a range of vegetation types: moist evergreen forest, moist semi-deciduous forest, freshwater inland swamp forest, forest regrowth and secondary/disturbed forest, farmbush, herbaceous swamps and floodplains. Commercial logging in Gola South was carried out in the periods 1963–1965 and 1975–1989. Since 1989, Gola has been subject to a conservation program. Outside of the protected areas, land cover is largely influenced by human activities and includes: disturbed and secondary forest, farmbush and shrubland/savanna, plantation, agriculture, bare soil, water courses and ponds.

In Liberia, the study area is sparsely populated and more forested. Verschuren (1983) indicated that the proposed Lofa-Mano Park (now referred to as Gola National Forest) covers a large area of evergreen rainforest in the south range, with semi-deciduous moist forest gradually taking over to the north, and with patches of low bush, marshes and some savannah on lateritic soil.

Overall, the area is characterized by a moist tropical climate with annual rainfall around 2500–3000 mm, a wet season lasting from May to October, and an altitude

in the range 70–410 m with no abrupt elevation changes. The dry period occurs between December and March, and corresponds to the semi-deciduous phenological stage of vegetation in the moist forest.

INSERT FIG. 1 HERE

2.2 Remote sensing data

We collected Landsat TM, ALOS AVNIR-2, and PALSAR scenes for image classification. The analysis of Landsat imagery from 1986 to the present day revealed cloud cover and haze over the area of interest in all seasons, as often reported for tropical forested regions (Asner, 2001). The best image, with respect to the time of field data collection was a Landsat TM scene from 15 January 2007, unevenly affected by haze and provided at level L1T (terrain corrected and projected in UTM zone 29N, Table 1, Fig. 2). This is coincident with the dry season and is therefore better suited for semi-deciduous vegetation detection. We acquired two AVNIR-2 scenes, dated 9 December 2009 (Table 1, Fig. 2), and three ALOS PALSAR FBD (Fine Beam Dual) scenes in slant range single look complex (SLC) format (Level 1.1), with pixel spacing 9.3 m in range and 2.7–4.5 m in azimuth, two being dated 22 June 2007 and one 24 August 2007 (Table 1, Fig. 3).

INSERT TABLE 1

2.3 Ground truth data acquisition

The ground truth was derived from field surveys realized in Sierra Leone and it was linked to the remotely-sensed images with the aid of visual interpretation.

Inside GRNP, 656 forest plots realized in 2006 were classified as having prevalence of evergreen or semi-deciduous tree species using TWINSPAN (Hill, 1979), a clustering algorithm for classifying species and samples. Outside the Park, a total of 872 land cover validation points were collected from 2008 to 2011, including: agriculture (including slash-and-burn, farmbush, and rice fields), plantations (oil palm and rubber), secondary/disturbed forest, undisturbed forest, burnt and urban areas, mining and water courses. These land cover/land use classes were re-organized as described in Table 2, thus incorporating the phenological information derived from the 2006 field survey (Klop et al., 2008).

INSERT TABLE 2

The surveys information allowed the selection of locations around which spectrally homogeneous Regions of Interest (ROIs) were digitized on screen. To mitigate any error introduced by temporal mismatching between remote sensing data and field surveys, and spatial mismatching caused by GPS inaccuracy, we selected only locations for which full agreement between available optical imagery and the field information was observed. We double-checked the selection of locations using also Google Earth very high resolution data, two Kompsat-2 (dated 17 April 2009) and three Ikonos (22 December 2009, 19 March 2006 and 19 February 2003), taking into account the differences on date acquisition between scenes. Cloud cover

presence over the images seriously limited the use of field information: a total of 208 locations were selected in the area covered by the TM image and 82 in the area covered by AVNIR-2, with most of the AVNIR-2 locations (70) coincident with those selected for TM data (Fig. 2). For Liberia, few forest locations were selected thanks to the data provided by GRNP staff and local experts (J. Lindsell, unpublished data). Different studies (Bayol and Chevalier, 2004; Shearman, 2009; World Bank 2011) have indicated the similarity between the Gola North block and the Liberian forests, with a majority cover of undisturbed forest.

INSERT HERE FIG. 2

The TM ROIs were subdivided into three parts: training (70%), validation (15%) and test (15%), for the purposes of classifying the TM and PALSAR scenes at 30 m spatial resolution, with the validation dataset used only in NN implementation. The dataset, initially different in amount for the various classes, was reduced in size by a random selection to obtain 2500 pixels for each land cover class. The ROIs are as evenly distributed as possible over the entire image; anyway a certain degree of spatial correlation occurs for water and oil palm plantation classes, due to their aggregated distribution in the study area and to limited accessibility.

Prior to define the 82 ROIs for the AVNIR-2 images, we checked over TM the coincident locations and ROIs digitized: TM ROIs were retained if they covered a spectrally and visually homogeneous area in AVNIR-2 image. When the finer spatial resolution of AVNIR-2 allowed for identification of more than one land

cover type inside a ROI, that region was either discarded, or else only the part of the ROI matching the indicated land cover was retained. As for TM, the ROIs were subdivided into three sets and randomly reduced to obtain 10000 pixels per land cover class, for the purposes of classifying the AVNIR-2 and PALSAR scenes at 10 m spatial resolution.

Statistical tests (not reported here) confirmed the absence of significant differences in the TM and AVNIR-2 ground truth for the various land cover classes, as well as in the different data sets used for training, validation and testing. With the described procedure we derived an AVNIR-2 ground truth as compatible as possible to the TM one while maintaining spectral purity, allowing for better understanding the performances of each sensor in classification tasks with respect to SAR integration.

INSERT HERE FIG 3

2.4 Remote sensing image preprocessing

Atmospheric corrections were performed on the TM and AVNIR-2 images to obtain the hemispherical directional reflectance factor (HDRF) using the Fast Line-of-Sight Atmospheric Analysis of Spectral Hypercubes (FLAASH) algorithm in ENVI version 4.7 (Exelis Visual Information Solutions, Boulder, Colorado). This is based on a MODTRAN4 approach for path scattered radiance, absorption, and adjacency effects (Felde et al., 2003). After atmospheric correction, haze was still detected on the TM image over the whole Sierra Leone area, while clearer

conditions characterized most of the Liberian side. Haze removal was attempted using the Haze Tool developed by Hu et al. (2009), which is a refinement of the haze optimized transformation (HOT) algorithm (Zhang et al., 2002; Zhang and Guindon, 2003). The corrected scene was less affected by uneven haze distribution, but still generated errors in classification results. Since the haze problem occurred in the visible bands, we excluded bands 1–3 of the TM image in our analysis.

An orthorectification based on a digital elevation model (DEM) from the ASTER derived Global Digital Elevation Map mission (GDEM, Tachikawa et al., 2011) was also performed on AVNIR-2 images. A mask was applied in order to exclude cloudy areas and cloud shadows, manually digitized on screen (Fig. 2). Then, the two AVNIR-2 scenes were mosaicked and co-registered to the TM scene (with Root Mean Square (RMS) of 0.51 at 30m pixel size), and eventually resampled to the original spatial resolution of 10 m. The AVNIR-2 mosaic covers only a portion of the study area due to cloud-masked zones and unavailability of an adjacent scene.

The FBD PALSAR images were multi-looked, terrain-corrected and geo-coded to a 15m spatial resolution using ASF (Alaska Satellite Facility) MapReady 3.0.6 and the aforementioned ASTER GDEM. SAR scenes were calibrated according to Shimada *et al*. (2009), mosaicked, co-registered to a TM image (RMS of 0.96 pixels) and then resampled twice to produce two scenes: one at 30 m to match

Landsat spatial resolution, and one at 10 m to match AVNIR-2. A Frost adaptive filter with a moderate window size of 5x5 was applied to the two SAR datasets (Fig. 3) to reduce speckle.

Our image analysis strategy was to combine either Landsat TM or AVNIR-2 with ALOS PALSAR in classification. Since the TM image and the PALSAR scenes do not overlay perfectly, we created subset images for TM and PALSAR corresponding to their area of overlap. The whole AVNIR-2 image falls within PALSAR, so there was no need to create a subset for it. Although the TM and AVNIR-2 images do not have equal area coverage, the ground truth for all classes is well represented in both images (Figs. 2 and 3).

2.5 Texture variables

Five texture variables including mean, entropy, correlation, variance, and second moment based on Grey-Level Co-Occurrence Matrix (GLCM) (Haralick, 1973) were created with ENVI version 4.7. Dorigo et al. (2012) describe extensively the GLCM texture characteristics and the need for selection of appropriate features and kernel size. We generated texture for the bands useful for vegetation detection (Asner, 1998), namely TM bands 4, 5, AVNIR-2 bands 3,4, plus for both ALOS PALSAR polarizations, using 64 grayscale quantization levels, 1 pixel shift and using 3x3, 5x5, 7x7, 9x9 and 15x15 window sizes. To reduce the number of features entering in classification a wrapper-based approach for texture variable

selection was here adopted. Several features selection methods exist, such as wrapper- and filter-based (Kohavi & John, 1997); filter-based methods are algorithms that use only training data to calculate the feature weights, whereas wrapper-based algorithms use feedback from a classifier to guide the search. We automated the comparison of the overall accuracies and Kappa coefficients obtained with MLC, using the training and validation ROIs specific for each dataset. We added one texture at a time to optical and SAR data, repeating the tests with increasing window size. We selected one variable for each band or channel, choosing the one that when added to the original data, produced the best classification result.

The automated procedure selected the following texture variables: for TM, entropy on band 4 and mean on 5 (9x9 window); for AVNIR-2, mean on bands 3 and 4 (15x15 window); for ALOS PALSAR, mean on both HH and HV polarizations (9x9 window). Any further increase in window size did improved classification accuracy. The selected window size of 9x9 for TM is well in agreement with other studies based on the same sensor (Li et al., 2012; Zhu et al., 2012).

2.6 Classification algorithms and selected tests

The Maximum likelihood classifier (MLC) is probably the most widely used parametric classifier (Richards and Jia, 1999), considered robust and still employed in recent forestry research (Herold et al., 2004; Lehmann et al., 2012; Lu et al., 2007; Rahaman and Sumantyo, 2010). It was here used to select texture features

and as benchmark classification algorithm for all tests. Among the most commonly used non-parametric classifiers is neural networks (NN), which has several advantages including its non-parametric nature, easy adaptation to different input data, learning and generalization capabilities (Lu and Weng, 2007), and is a rather competitive classifier even if compared with other sophisticated approaches (Pacifici et al., 2007; Licciardi et al., 2009). Atkinson (1997) reported that neural networks usually overcome typical problems experienced using parametric classifiers for land targets and are suitable for fusing multisource spatial data. Del Frate and Solimini (2004) critically analyzed NN in forestry problems, also in view of collinearity of inputs, observing that NN less suffers with respect to other algorithms from noise and saturation in L-band SAR data.

Here NN were used only for selected input combinations, with the aim of assessing the extent of improvement that a machine learning algorithm can bring in classification tasks. The NN were trained and tested with the same ground truth sets used in MLC classifications, while the validation dataset was used exclusively for NN implementation, avoiding the overfitting that results from the termination of the training phase when the error over the test dataset reaches a minimum (Bishop, 1995). The Conjugate Gradient (SGC; Moller, 1993) method was employed in the feed-forward neural networks. NN architecture was selected for each input dataset with a trial and error approach.

In our test strategy we first compared the classification accuracies obtained with MLC and NN algorithms on progressively complex inputs: 1) optical reflectance alone, 2) optical reflectance with its texture variables, 3) optical reflectance with its texture features, and SAR backscatter, and 4) optical reflectance, SAR backscatter, and texture variables from both. We repeated the tests over the TM and the AVNIR-2 datasets, thus exploring data integration with different optical datasets. Finally, we performed additional tests using SAR data alone, and with its derived textures, to assess its potential to support land cover mapping in areas persistently affected by clouds or haze and replace optical data. In these tests, we used two additional classification schemes by 1) merging two forest classes (secondary and semi-deciduous), and 2) merging all three classes (including evergreen) to reduce the complexity of the classification task and the number of land cover classes to be seven and six, respectively. Merged ROIs were randomly sampled to obtain again 2500 pixels per class. A list of the classification tests is reported in Table 3.

INSERT TABLE 3

Classification accuracies were assessed using overall accuracy, error matrix and Kappa coefficient of agreement (Cohen, 1960). The overall accuracy is the percentage of the correctly classified pixels in the validation dataset whereas the Kappa coefficient is a measure of the difference between the actual agreement and the chance agreement. The statistical differences in the Kappa coefficients of MLC and NN classifications at a 95% level of significance was determined using the Z-

test (Congalton and Green, 1999), which is performed for a pairwise comparison of the proposed methods and takes into account the ratio between the difference value of two Kappa coefficients and the difference of their respective variance.

3. Classification results

Optical data only: the MLC classification based on optical bands reached an overall accuracy of 80.4% for AVNIR-2 and 73.1% for TM (Table 4). The addition of texture selected variables to each type of image resulted in a noticeable increase in overall accuracy, with AVNIR-2 obtaining 93.7% and TM 85.7%. For TM, the increase in user accuracy was over 10% in all classes except bare soil/urban areas, already well discriminated by bands only (Table 4). The most significant increases with texture use are for oil palm plantation (30%), semi-deciduous forest (17%) and evergreen forest (14%), with respect to users accuracy. For AVNIR-2 the increase in user accuracy was more than 10 % for agriculture (14%), oil palm plantation (25%), secondary (32%) and semi-deciduous forest (15%) classes.

INSERT HERE TABLE 4

SAR data only: the overall accuracy of the MLC classification with SAR inputs (Table 5) was 49.9% and improved to 62.1% when using mean texture variables derived from both polarizations. Individual classes obtained a user accuracy increase between 6.3% and 35.1%, except in the case of water and farmbush (no change) and secondary forest (decrease due to confusion with other forest classes). According to users accuracies, texture was especially beneficial in detecting

evergreen forest (+ 28.7%), deciduous forest (+26.3%) and oil palm plantation (+35.1%). We obtained an overall accuracy of 64.5% when two forest types were merged, and of 75.7% when all forests were merged in a single class, thus with an increase of over 11% for a six classes land cover task.

INSERT HERE TABLE 5

Optical and SAR integrated data: SAR channels and their derived textures were concatenated to TM and AVNIR-2 datasets in two steps, first adding the channels only and then the selected textures parameters. The joint use of optical and SAR sensors increased overall accuracies (Table 6). When the TM bands 4–7 and their texture are used for MLC, the overall accuracy is 85.7% (Table 4); the addition of two PALSAR channels increases the accuracy to 89.5% and the further addition of PALSAR texture features increases it to 91.1%. For AVNIR-2, the pattern was similar, as the MLC of bands and texture leads to an overall accuracy of 93.7% (Table 4); the addition of PALSAR bands increases the accuracy to 94.1% and the further addition of PALSAR texture increases it to 95.6%. The use of SAR improved especially the agriculture (+8.6%) and farmbush classes (+12.3%) when added to TM data, as shown by users accuracies; when added to AVNIR-2 data, the increase was lower and distributed in all classes (Table 4 and Table 6). The use of SAR texture slightly changed the user accuracies from -0.4 to 4.3% with major benefits obtained for the semi-deciduous forest, evergreen forest and oil palm plantation classes.

INSERT HERE TABLE 6

Classification algorithms: the use of NN significantly increased accuracy of the results of optical data in the range 0.7–5.1% with respect to MLC according to Z statistics. With combined optical and SAR data, NN significantly increased results accuracy in the range 1.6–1.9% compared to MLC. For radar data as input, the use of NN increased overall accuracies from 1.1 to 3.3%, but the difference was significant only in one case. The increases brought by NN were not observed in any specific class but instead they were evenly distributed across all the land cover classes.

INSERT HERE TABLE 7

4. Discussion and conclusion

In the present study TM and AVNIR-2 optical datasets were used together with joined dual polarization SAR data to accurately classify a tropical area in West Africa, showing the effectiveness of integrating different data types in this complex region. The MLC classification map using TM near and shortwave infrared bands and SAR inputs is presented in Fig. 4 as the best result obtained with a freely available optical dataset and a widespread classification algorithm.

INSERT HERE FIG. 4

The distinction of different vegetation types is a task considered difficult due to the smooth transition between successional stages, such as farmbush (characterized by varying amounts of vegetation re-growth) and different forest types (Lucas et al., 2002; Vieira et al., 2003), and for the spectral similarity between evergreen and the

semi-deciduous classes, the latter often characterized by a leaf-drop period that could last only a few weeks. Vegetation-oriented classification efforts are especially needed in the region, where a trans-boundary peace park is planned by Liberia and Sierra Leone governments and conservation decisions are frequently taken. The integrated SAR-optical land cover map (Fig. 4) illustrates GRNP effectiveness, with the undisturbed forest classes mainly confined inside the park and toward Liberia. But it also shows the threat over the Gola South block, which is internally more fragmented than the other units and surrounded by anthropic pressure, and thus deserves special management attention.

We found that AVNIR-2 achieved a better result in classifying the eight land cover types, and especially the forest classes, with respect to spectrally reduced TM (bands 4,5,7). AVNIR-2 has a fine spatial resolution which allowed for capturing natural vegetation details (Table 4 and Fig. 4 (B)) and thus better represents environments characterized by mosaics of different vegetation and land cover types. Nevertheless, we still found a low separability of secondary and semi-deciduous classes (Table 4). Semi-deciduous forest mainly occurs in Gola South, where most selective logging took place until 1989. Accurate logging records are not available, but the indications are that these areas are still characterized by signs of old disturbances and thus share traits of secondary forest (Lindsall et al., in review). In our case study, as well as in other tropical environments, the distinction of forest types is useful for conservation while the mapping of the small forest

patches outside reserves is also valuable for management, as their change in extension is a tool to assess the value of community forests as carbon sinks and the effectiveness of financial compensation schemes.

While the discrimination of the eight land cover/land use types of the study area was a difficult task for the PALSAR sensor alone, when the three forests classes were merged (thus reducing the task to six classes) the SAR classification accuracy reached 75.7 % (Table 5). The SAR based map allows for clear detection of the forested areas (Fig. 5). Confusion between forest and later-stage farmbush and overestimation of the oil palm plantation class is observable, due to similarity of their vertical structure at L-band. In a similar way we observed confusion between early-stage farmbush and agriculture, both having lack of woody components. Anyway, this result goes beyond the usual SAR-based forest/non-forest mapping and the obtained accuracy value is similar or higher than other classifications based on SAR in African environments (Haack and Bechdol, 2000; Herold et al., 2004). As in our case, with both optical images impacted by atmospheric conditions (clouds or haze), is frequent to experience optical data unavailability in tropical regions. The loss of information on forests details, with respect to classification based on integrated optical and SAR data, was counterbalanced by full SAR coverage of the area. The use of SAR is suggested as a strategy to cope with persistent cloud cover affecting tropical regions: in this study we showed that SAR alone can still provide important landscape information. Furthermore, it is the SAR

combination with optical data –TM or AVNIR-2 – that always produces the best outputs (Table 6). This result confirms SAR role in forest and vegetation mapping of tropical regions, and suggests that in areas affected by optical data loss different optical resolutions can be exploited and joined with SAR. If available, finer resolution sensors such as AVNIR-2 can help to detail specific sub-areas of interest, while larger areas or zones covered by clouds can be filled with SAR or optical lower resolution data.

With regards to the techniques here tested here to improve the mapping accuracy, we found that the addition of the optical texture features was very effective in improving the classification results in all cases, with an increase between 10.1% and 13.2%. The result shows that the reflectance differences and the shadow effects occurring in different forest types can be partially captured by optical texture measures. The addition of SAR texture variables increased the accuracies significantly in SAR-only tests, similarly to what has been found by Longepe et al. (2011) in tropical forests, again confirming the value of textural information when this data type is used singularly, and especially for discriminating classes of dense and tall vegetation (Table 5). On the other hand, SAR texture was much less effective when included as the last input to optical, optical texture and SAR datasets (Table 7), perhaps due to the fact that very high values of accuracy were already reached and thus the margins of improvement were limited.

The use of the NN algorithm brought in an improvement in the results with respect to MLC. This improvement is limited when SAR and optical data are integrated (1.6 – 1.9%) and not significant in most classifications based on SAR data only (Table 7). The decision to adopt machine learning should take into consideration the need for expert knowledge, evaluating its cost against the amount of improvement obtained in classification. In this respect we found that the NN accuracy increase was beneficial but limited in amount, partially due to the high values already obtained by MLC, thus suggesting the machine learning adoption as an added tool only when resources allows for it.

A key constraint for implementing monitoring systems at a fine scale is the availability of finer resolution data (Achard et al., 2010). In this view, this research showed the improvement observed with the spatial resolution of AVNIR-2 sensors and its successful integration with a coarser SAR data. The atmospheric conditions in the moist tropical regions pose another serious challenge for data availability. Until new sensors are available, with increased revisiting capabilities, it is fundamental to exploit and integrate the few available data to accurately classify the landscape of those remote areas. This research tested a possible approach in a complex environment, and similar efforts can be easily replicated in the region to first map and then monitor the growing number of conservation units.

Techniques to mosaic multi-date images at a pixel level are an option for helping to solve the problem of cloud cover (Roy et al., 2010). The use of multi-temporal SAR datasets is also known to improve accuracy of results (Ranson and Sun, 1994; Chen et al., 1996) and another promising approach is the integration of microwave frequencies (e.g. at L- and C-band; Lardeux et al., 2011), which should be able to provide information both on foliage strata, helpful in the distinction of different canopies structure and vegetation water content, and on forest volumes, which are related to disturbance and age. While waiting for new data from future generation optical and SAR space missions, the adoption of these existing techniques and datasets could offer improved mapping capabilities and will represent our future research step for tropical complex regions.

5. Acknowledgements

Landsat TM data were obtained from the GLOVIS service of the U.S. Geological Service (USGS). ALOS AVNIR-2 and Kompsat-2 scenes were obtained from the European Space Agency (ESA) through a Category 1 Proposal (C1P 7500). The GeoEye Foundation provided the Ikonos images through a grant. ALOS PALSAR scenes were obtained through an Alaska Satellite Facility grant (ID 588). We acknowledge the ERC grant Africa GHG #247349 and the Cambridge Conservation Initiative for providing additional support to the investigation.

References

Achard, F., Stibig, H-J., Eva, H.D., Lindquist, E.J., Bouvet, A., Arino, O., Mayaux, P., 2010. Estimating tropical deforestation from Earth observation data. *Carbon Management*, 1(2), 271-287.

Asner, G.P., 1998. Biophysical and Biochemical Sources of Variability in Canopy Reflectance. *Remote Sensing of Environment*, 64(3), 234-253.

Asner, G. P., 2001. Cloud cover in Landsat observations of the Brazilian Amazon. *International Journal of Remote Sensing*, 22(18), 3855-3862.

Atkinson, P. M., Tatnall, A.R.L., 1997. Neural networks in remote sensing. *International Journal of Remote Sensing*, 18(4), 699-709.

Avitabile, V., Baccini, A., Friedl, M.A., Schmullius, C., 2012. Capabilities and limitations of Landsat and land cover data for aboveground woody biomass estimation of Uganda. *Remote Sensing of Environment*, 117, 366-380.

Bayol, N., Chevalier, J.F., 2004. Current state of the forest cover in Liberia –forest information critical to decision making, Forest Resources Management. Study report for the World Bank, 25 June 2004.

Berberoglu, S., Lloyd, C.D., Atkinson, P.M., Curran, P.J., 2007. Texture classification of Mediterranean land cover. *International Journal of Applied Earth Observation and Geoinformation*, 9(3), 322-334.

Bishop, C.M., 1995. *Neural Networks for Pattern Recognition*. Oxford University Press, Oxford.

Buckland, S.T., Anderson, D.R., Burnham, K.P., Laake, J.L., Borchers, D.L., Thomas, L. (Eds.), 2004. *Advanced Distance Sampling*. Oxford University Press, Oxford. 414pp.

CEPF, 2003. *Critical Ecosystem Partnership Fund. Guinean Forests of West Africa Hotspot Upper Guinean Forest Briefing Book*. Prepared for: Improving Linkages Between CEPF and World Bank Operations, Africa Forum, Cape Town, South Africa—April 25 – 27, 2005

Chan, J. C.-W., Laporte, N., Defries, R.S., 2003. Texture classification of logged forests in tropical Africa using machine learning algorithms. *International Journal of Remote Sensing*, 24(6), 1401-1407.

Chen, D., Stow, D.A., Gong, P., 2004. Examining the effect of spatial resolution and texture window size on classification accuracy: an urban environment case. *International Journal of Remote Sensing*, 25(11), 2177-2192.

Chen, K. S., W. P. Huang, D. H. Tsay, Amar, F., 1996. Classification of multi-frequency polarimetric SAR imagery using a dynamic learning neural network. *IEEE Transactions on Geosciences and Remote Sensing*, 34(3), 814-820.

Chica-Olmo, M., Abarca-Hernandez, F., 2000. Computing geostatistical image texture for remotely sensed data classification. *Computers and Geosciences*, 26(4), 373-383.

Cohen, J., 1960. A coefficient of agreement for nominal scales, *Educational and Psychological Measurement*, 20, 37-46.

Cole, N.H.A., 1993. Floristic association in the Gola rain forests: a proposed biosphere reserve. *Journal of Pure and Applied Science*, 2, 35-50.

Congalton, R., Green, K., 1999. *Assessing the Accuracy of Remotely Sensed Data: Principles and Practices*, CRC/Lewis Press, Boca Raton, FL.

Del Frate, F., Solimini, D., 2004. On a neural network algorithm for retrieving forest biomass from SAR data. *IEEE Transactions on Geoscience and Remote Sensing*, 42, 24-34.

Dekker, R. J., 2003. Texture analysis and classification of ERS SAR images for Map updating of urban areas in the Netherland. *IEEE Transactions on Geoscience and Remote Sensing*, 41(9), 1950–1958.

Dorigo, W., Lucieer, A., Podobnikar, T, Carni, A., 2012. Mapping invasive Fallopia japonica by combined spectral, spatial, and temporal analysis of digital orthophotos. *International Journal of Applied Earth Observation and Geoinformation* 19, 185–195.

Erasmi, S., Twele, A., 2009. Regional land cover mapping in the humid tropics using combined optical and SAR satellite data: a case study from Central Sulawesi, Indonesia. *International Journal of Remote Sensing*, 30(10), 2465-2478.

Felde, G.W., Anderson, G.P., Cooley, T.W., Matthew, M.W., Adler-Golden, S.M., Berk, A., Lee, J., 2003. Analysis of Hyperion Data with the FLAASH Atmospheric Correction Algorithm. *Proceedings of the International Geoscience and Remote Sensing Symposium*, Toulouse, France, (IGARSS'03), 90-92.

Gibbs, H.K., Brown, S., Nilesand, J.O., Foley, J.A., 2007. Monitoring and estimating tropical forest carbon stocks: making REDD a reality. *Environmental Research Letters*, 2(4), 1-13.

Haack, B., Bechdol, M., 2000. Integrating multisensor data and radar texture measures for land cover mapping, *Computers and Geosciences*, 26(4), 411-421.

Haralick, R. M., Shanmugan, K., Dinstein, I., 1973. Textural Features for Image Classification, *IEEE Transactions on Systems, Man, and Cybernetics*, 3(6), 610-621.

Herold, N.D., Haack, B.N. Solomon E., 2004. An evaluation of radar texture for land use/cover extraction in varied landscapes. *International Journal of Applied Earth Observation and Geoinformation*, 5(2), 113–128.

Hill, M.O., 1979. TWINSPAN--A FORTRAN program for arranging multivariate data in an ordered two-way table by classification of the individuals and attributes. Ithaca, NY: *Ecology and Systematics*, Cornell University.

Hu, J., Chen, W., Li, X., He, X., 2009. A haze removal module for multispectral satellite imagery. *Urban Remote Sensing Joint Event*, Shanghai, China, (JURSE 2009), 4p.

Igue, A.M., Houndagba, C.J., Gaiser, T., Stahr, K., 2006. Land Use/Cover Map and its Accuracy in the Oueme Basin of Benin (West Africa). *Conference on International Agricultural Research for Development*, Bonn, Germany, (Tropentag), 4p.

Judex,M., Thamm, H. P., Menz, G., 2006. Improving land cover classification with knowledge based approach and ancillary data. *Proceedings of the 2nd Workshop of the EARSeL SIG on Land Use and Land Cover*.

Klop, E., Lindsell J., Siaka A., 2008. Biodiversity of Gola Forest, Sierra Leone. Royal Society for the Protection of Birds, Conservation Society of Sierra Leone, Government of Sierra Leone.

Kohavi, R., John, G.H., 1997. Wrappers for feature subset selection. *Journal of Artificial Intelligence*, 97(1-2), 273-324.

Kuplich, T.M., 2006. Classifying regenerating forest stages in Amazonia using remotely sensed images and a neural network. *Forest Ecology and Management*, 234(1-3), 1-9.

Lardeux, C., Frison, P.-L., Tison, C., Souyris, J.-C., Stoll, B., Fruneau, B., Rudant, J.-P., 2011. Classification of Tropical Vegetation Using Multifrequency Partial SAR Polarimetry. *IEEE Geoscience and Remote Sensing Letters*, 8, 133-137.

Li, G., Lu, D., Moran, E.F., Hetrick, S., 2011. Land-cover classification in a moist tropical region of Brazil with Landsat Thematic Mapper imagery. *International Journal of Remote Sensing*, 32(23), 8207-8230.

Licciardi, G. , Pacifici, F., Tuia, D., Prasad, S., West, T., Giacco, F., Thiel, C., Inglada, J., Christophe, E., Chanussot, J., Gamba, P., 2009. Decision Fusion for the Classification of Hyperspectral Data: Outcome of the 2008 GRS-S Data Fusion Contest, *IEEE Transaction on Geoscience and Remote Sensing*, 47(11), 3857 - 3865.

Lefsky, M.A., Cohen, W.B., 2003. Selection of remotely sensed data. In: Wulder, M.A., Franklin, S.E. (Eds.), *Remote Sensing of Forest Environments: Concepts and case studies*, Kluwer Academic Publishers, Boston, pp. 13-46.

Lehmann, E. A., Caccetta, P.A., Zhou, Z., McNeill, S.J., Wu, X., Mitchell, A.L., 2012. Joint Processing of Landsat and ALOS-PALSAR Data for Forest Mapping and Monitoring. *IEEE Transactions on Geoscience and Remote Sensing*, 50, 55-67.

Longepe, N., Rakwatin, P., Isoguchi, O., Shimada, M., Uryu, Y., Yulianto, K., 2011. Assessment of ALOS PALSAR 50 m Orthorectified FBD Data for Regional Land Cover Classification by Support Vector Machines. IEEE Transactions on Geoscience and Remote Sensing, 49(6), 2135-2150.

Lu, D., Weng, Q., 2007. A survey of image classification methods and techniques for improving classification performance. *International Journal of Remote Sensing* 28(5), 823-870.

Lu, D., Batistella, M., Moran, E., 2007. Land-cover classification in the Brazilian Amazon with the integration of Landsat ETM+ and RADARSAT data. *International Journal of Remote Sensing*, 28 (24), 5447–5459.

Lucas, R. M., Honzák, M., Amaral, I. D., Curran, P. J., Foody, G.M. (2002). Forest regeneration on abandoned clearances in central Amazonia. *International Journal of Remote Sensing*, 23(5), 965-988.

Mitchard, E.T.A., Saatchi, S.S., White, L.J.T., Abernethy, K.A., Jeffery, K.J., Lewis, S. L., Collins, M., Lefsky, M.A., Leal, M.E., Woodhouse, I.H., Meir, P. (2011). Mapping tropical forest biomass with radar and spaceborne LiDAR: overcoming problems of high biomass and persistent cloud. *Biogeosciences*, 8(4), 8781-8815.

Moller, M. F., 1993. A scaled conjugate gradient algorithm for fast supervised learning. *Neural Networks*, 6(4), 525-533.

Pacifici, F., Del Frate, F., Emery, W.J., Gamba, P., Chanussot, J., 2002. Urban mapping using coarse SAR and optical data: outcome of the 2007 GRS-S data fusion contest, *IEEE Geoscience and Remote Sensing Letters*, 5(3), 331-335.

Price, K., Guo, X., Stiles, J.M., 2002. Optimal Landsat TM band and vegetation indices for discrimination of six grassland types in eastern Kansas. *International Journal of Remote Sensing*, 23(23), 5031-5042.

Quattrochi, D.A., Goodchild, M.F. (Eds), 1997. *Scale in Remote Sensing and GIS*. Lewis Publishers, New York.

Rahman, M.M., Sumantyo J.T.S., 2010. Mapping tropical forest cover and deforestation using synthetic aperture radar (SAR) images. *Applied Geomatics*, 2(4), 113-121.
Ranson, K. J., Sun G., 1994. Northern forest classification using temporal multifrequency and multipolarimetric SAR images. *Remote Sensing of Environment*, 47(2), 142-153.

Richards, J.A., Jia, X., 1999. *Remote Sensing Digital Imaging Analysis: an Introduction*, third ed. Springer, Berlin.

Roy, D. P., Ju, J., Kline, K., Scaramuzza, P. L., Kovalskyy, V., Hansen, M., Loveland, T.R., Vermote, E., Zhang, C., 2010. Webenabled Landsat data (WELD): Landsat ETM+ composited mosaics of the conterminous United States. *Remote Sensing of Environment*, 114, 35−49.

Santos, J.R., Neeff, T., Dutra, L.V., Araujo, L.S., Gama, F.F., Elmiro, M.A.T., 2004. Tropical forest biomass mapping from dual frequency SAR interferometry (X and P-Bands). *Twentieth International Society for Photogrametry and Remote Sensing (ISPRS)* Congress: GeoImagery Bridging Continents, Istanbul, v.XXXV, pp. 1133-1136.

Shearman, P.H., 2009. An Assessment of Liberian Forest Area, Dynamics, FDA Concessions Plans, and their Relevance to Revenue Projections, Rights and Resources Initiative.

Shimada, M., Isoguchi, O., Tadono, T., Isono, K., 2009. PALSAR radiometric and geometric calibration. *IEEE Transactions on Geosciences and Remote Sensing*, 47(12), 3915-3932.

Simard, M., Saatchi, S., De Grandi. G.F., 2000. The use of decision tree and multiscale texture for classification of JERS-1 SAR data over tropical forest. *IEEE Transactions on Geoscience and Remote Sensing*, 38(5), 2310-2321.

Tachikawa, T., Kaku, M., Iwasaki, A., Gesch, D., Oimoen, M., Zhang, Z., Danielson, J., Krieger, T., Curtis, B., Haase, J., Abrams, M., Crippen, R., Carabajal., C., 2011. ASTER Global Digital Elevation Model Version 2 – Summary of Validation Results. ASTER GDEM Validation Team: METI/ERSDAC NASA/LPDAAC USGS/EROS.

Talavera, L., 2005. An evaluation of filter and wrapper methods for feature selection in categorical clustering. *6th International Symposium on Intelligent Data Analysis* (IDA05), pp.440–451.

Toll, D.L., 1985. Effect of Landsat Thematic Mapper sensor parameters on land cover classification. *Remote Sensing of Environment*, 17(2), 129-140.

Verschuren, J., 1983. Conservation of tropical rain-forest in Liberia: recommendations for wildlife conservation and national parks. Report prepared for IUCN, Gland, Switzerland

Vieira, I.C.G., Almeida, A.S., Davidson, E.A., Stone, T.A., Carvalho, C.J.R., Guerrero, J.B., 2003. Classifying successional forests using Landsat spectral properties and ecological characteristics in eastern Amazônia. *Remote Sensing of Environment*, 87(4), 470-481.

Wijaya A, Marpu PR, Gloaguen R., 2008. Geostatistical texture classification of tropical rainforest in Indonesia. In: J.S. Alfred Stein, and Wietske Bijker (Eds.), *Quality Aspect in Spatial Data Mining* (pp. 199–210). CRC Press Inc.

World Bank, 2011. Forest Resource Assessments in Liberia. Report on field verification. River Cess County, Liberia. Michael Abedilartey.

Yavitt, J.B., Battles, J.J., Lang, G.E., Knight, D.H., 1995. The canopy gap regime in a secondary Neotropical forest in Panama. *Journal of Tropical Ecology*, 11(3), 391-402.

Zhang, Y., Guindon, B., Cihlar J., 2002. An image transform to characterize and compensate for spatial variations in thin cloud contamination of Landsat images. *Remote Sensing of Environment*, 82(2-3),173-187.

Zhang, Y., Guindon, B., 2003. Quantitative assessment of a haze suppression methodology for satellite imagery: Effect on land cover classification performance. *IEEE Transactions on Geoscience and Remote Sensing*, 41(5), 1082-1089.

Zhu, Z., Woodcock, C. E., Rogan, J., Kellndorfer J., 2012. Assessment of spectral, polarimetric, temporal, and spatial dimensions for urban and peri-urban land cover classification using Landsat and SAR data. *Remote sensing of Environment*, 117, 72-82.

Table 1**.** Summary of remote sensing data used in the research.

Sensor	Dates	Data characteristics
Landsat TM	15 Jan. 2007	30x30 m spatial resolution, 7 spectral bands Band 1: 0.45 - 0.52 m (Blue); Band 2: 0.52 - 0.60 m (Green); Band 3: 0.63 - 0.69 m (Red); Band 4: 0.76 - 0.90 m (Near infrared); Band 5: 1.55 - 1.75 m (Short wave infrared); Band 6: 10.4 - 12.5 m (Thermal infrared); Band 7: 2.08 - 2.35 m (Short wave infrared). L1T product. Thermal band neglected.
ALOS PALSAR	22 June 2007 24 Aug 2007	SAR L-band in HH and HV polarization. FBD Level 1.1 product: Single Look Complex provided in slant range geometry
ALOS AVNIR-2	9 Dec. 2009	10x10 m spatial resolution, 4 spectral bands Band 1 : 0.42 to 0.50 m Band 2 : 0.52 to 0.60 m Band 3 : 0.61 to 0.69 m Band 4 : 0.76 to 0.89 m Level 1B2 product.

Table 2. Characteristics of the selected land use classes and forest physiognomies.

Secondary (degraded) forest (SF)	characterized by trees with height > 5 m, sometimes with presence of understory crops (coffee, cocoa), canopy cover > 20%, evidence of human disturbance, logging history, >15–20 years from regeneration if cleared
Farmbush/Shrubland/Savanna (FB)	dominated by non-tree vegetation such as shrubs and/or grasses, canopy cover < 20%, agriculture can be present but should not occupy more than 25% of the area, trees usually less than 5 m tall. Can be land which has been abandoned after shifting cultivation occurred few years before (< 15–20)
Plantation (OP)	dominated by oil palm or rubber, evidence of human activity, canopy cover >20%, tree height > 5 m
Agriculture (AG)	dominated by specific crops such as rice on irrigated soil, usually found in small patches, evidence of human activity
Bare soil/Urban areas (BS)	represented by villages, open areas not yet cultivated or exposed substrate with little or no vegetation, including recently burned land
Evergreen forest (EF)	tree height > 5 m and canopy cover > 60%, no evidence of human disturbance
Semi-deciduous forest (DF)	tree height > 5 m and canopy cover > 60%, no evidence of human disturbance, presence of semi-deciduous species
Water (W)	rivers, water courses and ponds

Table 3. Datasets used as classification inputs and tested with MLC and/or NN approaches.

Optical data
1) TM bands 4,5,7
2) TM bands 4,5,7 + texture (entropy b4, mean b5; 9x9 window)
3) AVNIR-2 all bands
4) AVNIR-2 all bands + texture (mean b3, mean b4; 15x15 window)
SAR data
5) ALOS PALSAR HH-HV bands
6) ALOS PALSAR HH-HV bands + texture (mean HH, mean HV; 9x9 window)
Combined SAR + optical data
7) TM bands 4,5,7 + texture + PALSAR HH HV
8) TM bands 4,5,7 + TM texture + PALSAR HH HV + PALSAR texture
9) AVNIR-2 + texture + PALSAR HH HV
10) AVNIR-2 + texture + PALSAR HH HV + PALSAR texture

Table 4. Classification results for optical data obtained with MLC. PA = Producer Accuracy; UA = User Accuracy; OA = Overall Accuracy; KC = Kappa Coefficient

Land cover class	TM bands 4,5,7		TM bands 4,5,7 + TM texture		AVNIR-2 bands		AVNIR-2 bands + AVNIR-2 texture	
	PA%	UA%	PA%	UA%	PA%	UA%	PA%	UA%
AG	59.6	73.6	76	84.3	93.8	80.3	96.6	95.1
BS	99.6	99.3	100	99.6	82.2	96.7	98.3	99.1
EF	65.3	72.6	89.3	87	81.4	78.7	92.5	87
FB	81	68.9	86.6	81	85.2	87.1	95.4	94
OP	84.9	65.3	94.6	95.3	88.8	70.7	96.2	96.3
SF	38.6	57.6	65	70.3	36.6	56	80.8	88.9
DF	62.9	54.3	78	71.6	76.3	71.3	90.4	89
W	97.6	100	98.3	100	99	100	99.2	100
OA%	73.1		85.7		80.4		93.7	
KC	0.69		0.83		0.77		0.92	

Table 5. Classification results for SAR data obtained with MLC. PA = Producer Accuracy; UA = User Accuracy; OA = Overall Accuracy; KC = Kappa Coefficient

	PALSAR HH HV		PALSAR HH HV + texture			PALSAR HH HV + texture 7 classes			PALSAR HH HV + texture 6 classes	
Land cover class	PA%	UA%	PA%	UA%	Land cover class	PA%	UA%	Land cover class	PA%	UA%
AG	43.3	47.9	58.6	57.6	AG	58.0	59.0	AG	57.6	58.9
BS	56.6	69.6	87.0	75.9	BS	75.9	87.0	BS	75.0	87.0
EF	52.3	32.6	43.3	61.3	EF	90.0	49.6	EF+SF+DF	76.0	68.9
FB	42.0	48.6	63.3	48.3	FB	49.6	66. 3	FB	89.0	76.0
OP	72.0	50.9	72.6	86.0	OP	86.3	71.9	OP	53.3	73.9
SF	8.6	38.6	37.6	17.3	SF+DF	4.6	25.9	W	86.3	97.3
DF	43.6	34.6	45.6	60.9	W	91.9	74.3			
W	87.3	95.3	97.3	95.3						
OA%	49.9		62.1		OA%	64.5		OA%	75.7	
KC	0.42		0.56		KC	0.58		KC	0.70	

Table 6. Classification results for joined optical and data obtained with MLC. PA = Producer Accuracy; UA = User Accuracy; OA = Overall Accuracy; KC = Kappa Coefficient

	TM b4,5,7 + TM texture + PALSAR		TM b4,5,7 + TM texture + PALSAR + PALSAR texture		AVNIR-2 + AVNIR-2 texture + PALSAR		AVNIR-2 + AVNIR-2 texture + PALSAR + PALSAR texture	
Land cover class	PA%	UA%	PA%	UA%	PA%	UA%	PA%	UA%
AG	91.6	92.9	94.6	93.9	97.4	95.3	97.6	96.6
BS	100.0	100.0	100.0	99.6	97.8	99.4	98.8	99.5
EF	89.3	88.6	90.0	91.0	92.9	87.8	94.6	92.1
FB	93.0	93.3	93.6	95.0	95.8	94.6	96.4	94.8
OP	97.9	96.0	99.6	98.9	96.8	97.1	98.0	98.3
SF	69.6	73.6	70.9	77.6	81.7	89.4	85.7	93.1
DF	78.0	74.3	82.3	75.0	91.2	89.4	94.0	90.5
W	98.6	95.3	99.3	95.3	99.4	100.0	99.8	100.0
OA%	89.5		91.1		94.1		95.6	
KC	0.88		0.89		0.93		0.95	

Table 7. Comparison of results obtained with ML and NN, network architecture (hidden layers and neurons used) and Z statistics scores. The asterisk indicates results which are not significant at the 5 % confidence level.

	Overall Accuracy				
Landsat TM	ML	NN	hidden layers	neurons	Z score
TM 4,5,7 bands	73.1	74.0	2	32	2.16
TM 4,5,7 bands + TM texture	85.7	90.8	2	54	-6.03
TM 4,5,7 bands + TM texture + PALSAR	89.5	91.4	2	32	-2.34
TM 4,5,7 bands + TM texture + PALSAR + PALSAR texture	91.1	92.7	2	54	2.2
AVNIR					
AVN bands	80.4	81.5	2	32	-1.98
AVN bands + texture	93.7	94.4	2	32	-2.16
AVN bands + texture + PALSAR	94.1	95.8	1	24	6.05
AVN bands + texture + PALSAR + PALSAR texture	95.6	97.5	2	32	-5.33
ALOS PALSAR					
HH HV	49.9	51.1	2	18	-0.89*
HH HV + texture	62.1	63.8	2	32	-1.35*
HH HV + texture 7 classes	64.5	67.8	2	32	2.54
HH HV + texture 6 classes	75.7	78.1	2	32	-1.89*

List of Figures.

Fig. 1. Location of the study area; protected areas are shown in green. Area covered by TM and ALOS PALSAR data is shown in blue and by AVNIR-2 in red.

Fig. 2. Left: Landsat TM 2007 false color image (Red: band 7, Green: band 4, and Blue: band 3) cut to match the area in common with ALOS PALSAR. Right: AVNIR-2 cloud-masked true color image (Red: band 3, Green: band 2, and Blue: band 1), where the black areas are affected by cloud and thus manually masked out. The Gola Rainforest National Park and Tiwai Island Wildlife Reserve boundaries are shown in red. The locations where ROIs have been generated are shown as red points in both images.

Fig. 3. Left: Three ALOS PALSAR mosaicked scenes (two dated 22 June 2007 and one 24 August 2007) 30 m pixel size, masked over the area common to the Landsat image. Right: Three ALOS PALSAR mosaicked scenes, 10 m pixel size, masked over the area common to the AVNIR-2 image. Both are false color composites (Red: HH, Green: HV, Blue: difference HH-HV). The Gola Rainforest National Park and Tiwai Island Wildlife Reserve boundaries are shown in red.

Fig. 4. Land cover classification map obtained with MLC and input 'TM bands 4,5,7 + TM Textures + PALSAR HH HV + PALSAR Textures'. The black box in the main figure (A) delimits a small area of the TM classification map shown in close up in (B); the same area as seen in the classification based on AVNIR-2 (C) (input 'AVNIR-2 + AVNIR-2 textures + SAR + SAR textures'). The Gola Rainforest National Park and Tiwai Island Wildlife Reserve boundaries are shown in red.

Fig. 5. Land cover classification map obtained with MLC and input 'ALOS PALSAR HH HV + texture 6 classes. The Gola Rainforest National Park and Tiwai Island Wildlife Reserve boundaries are shown in red.

Figure

Click here to download high resolution image

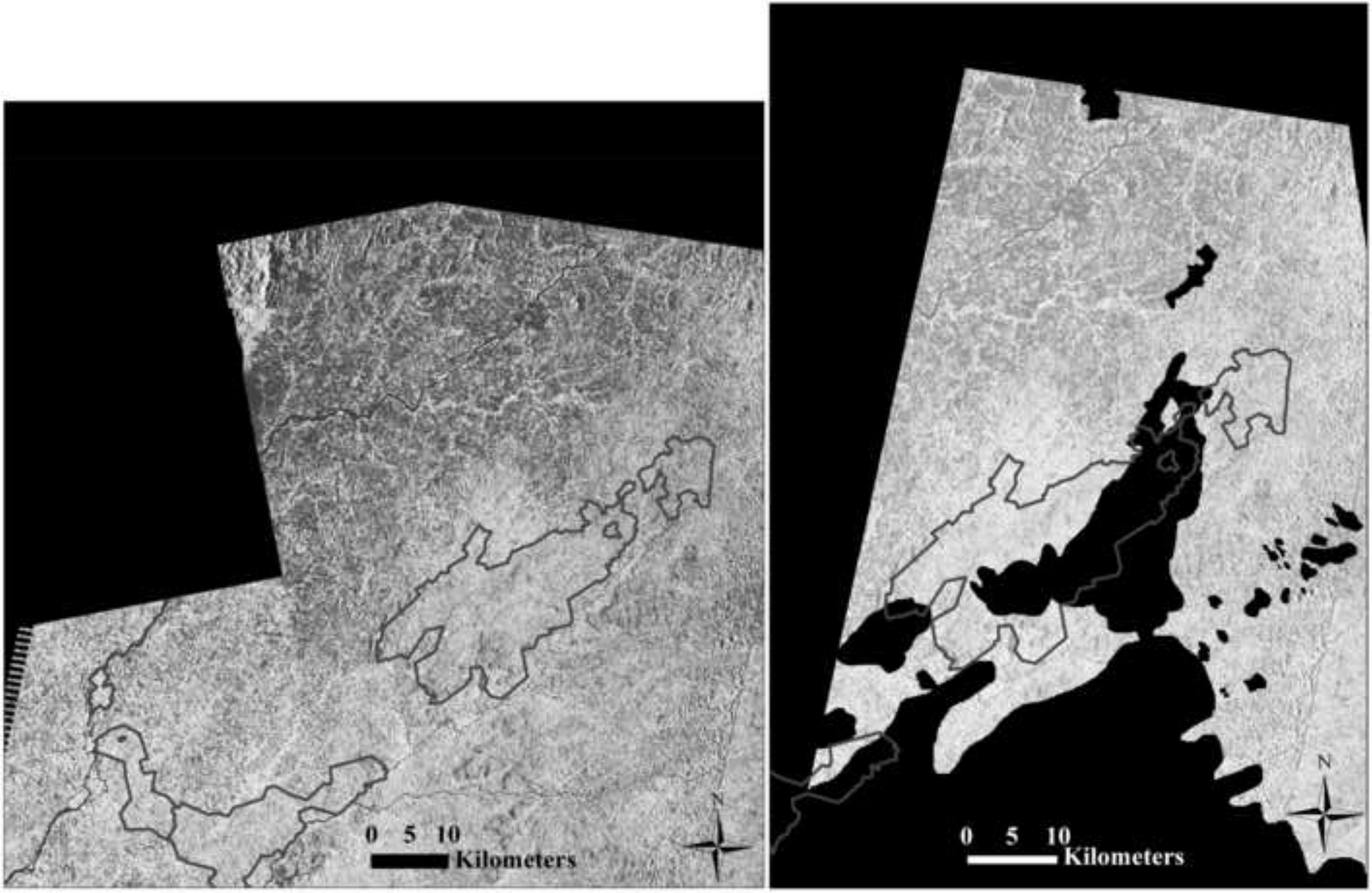

Figure

Click here to download high resolution image

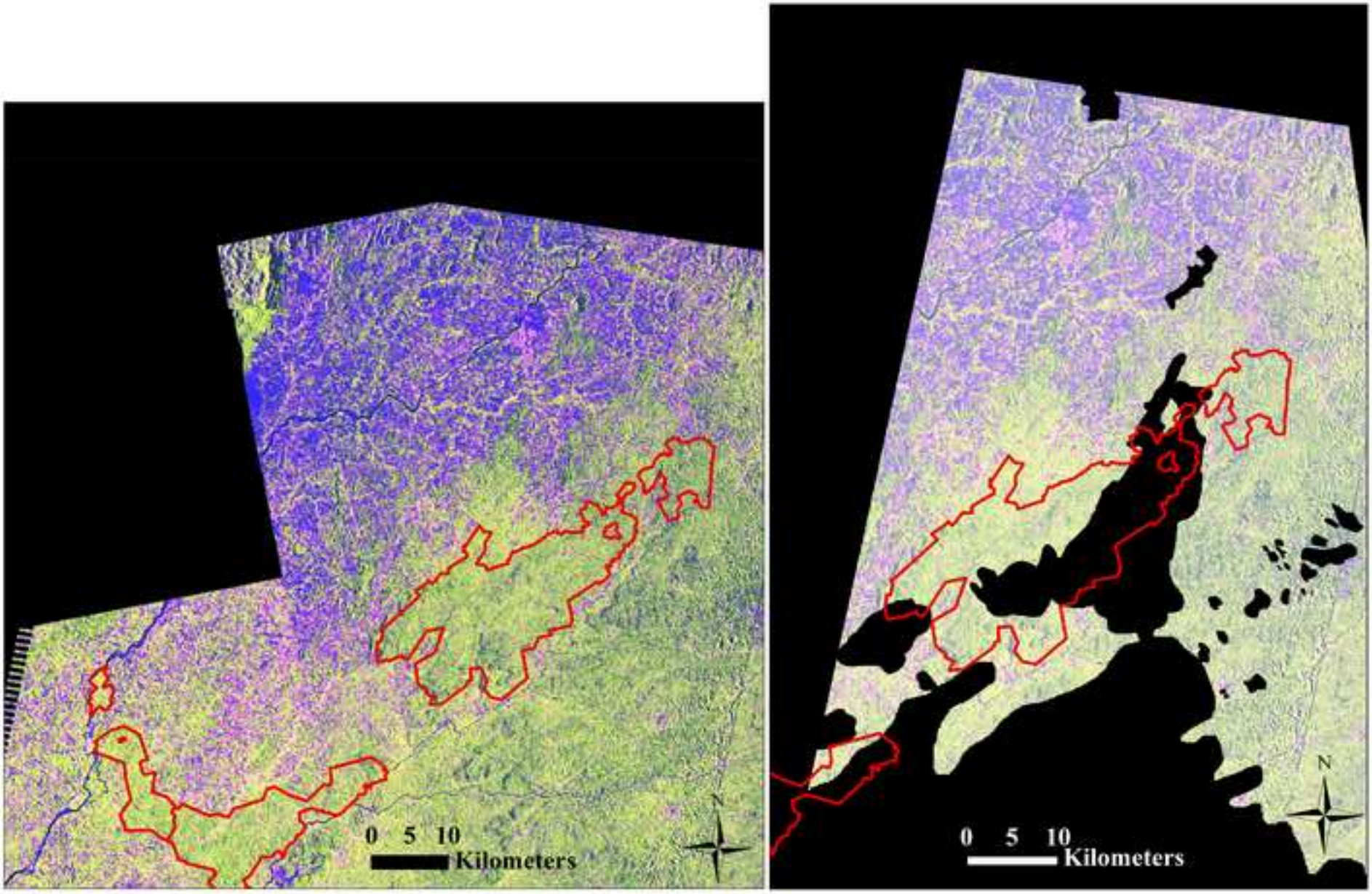

Figure

Click here to download high resolution image

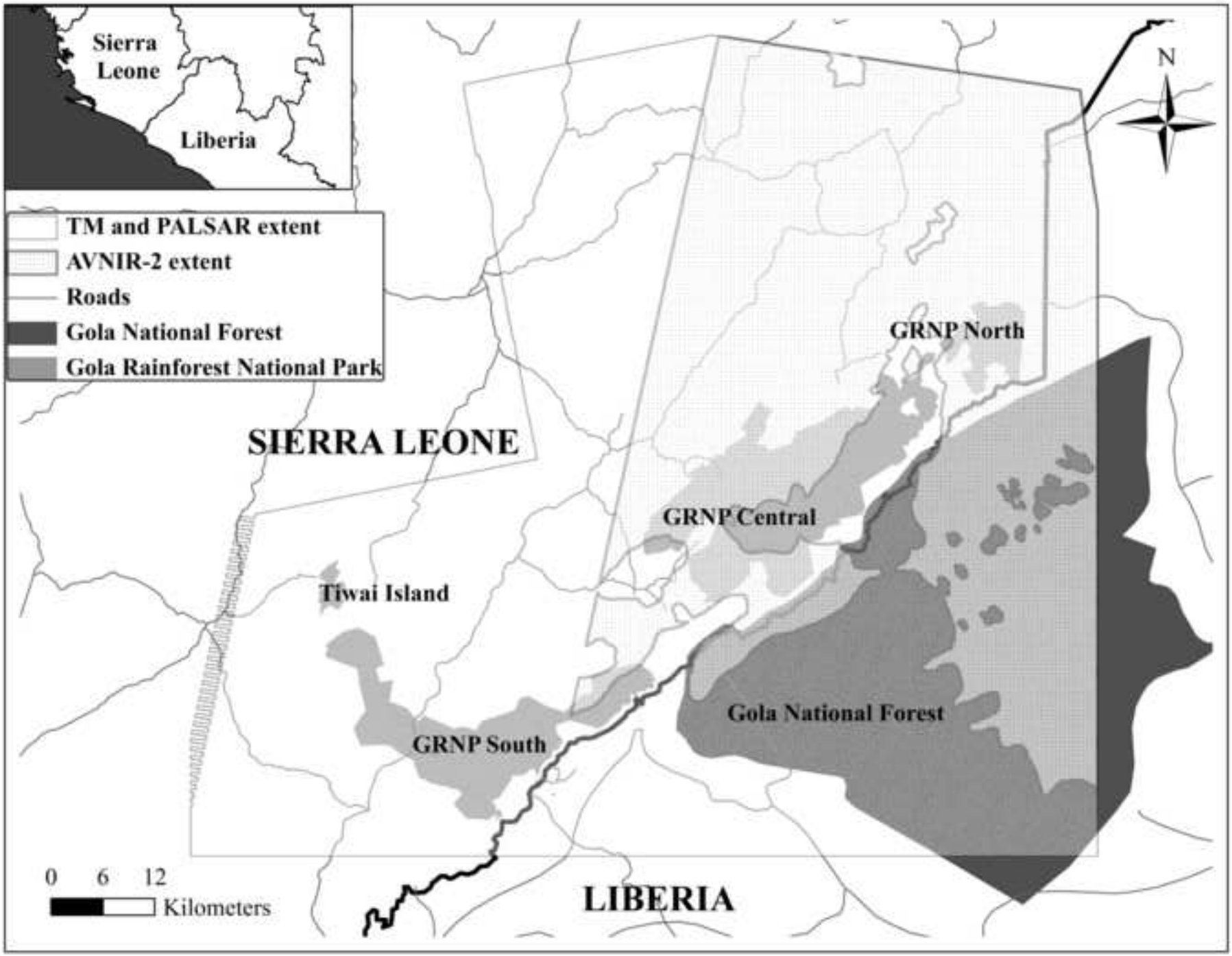

Figure

Click here to download high resolution image

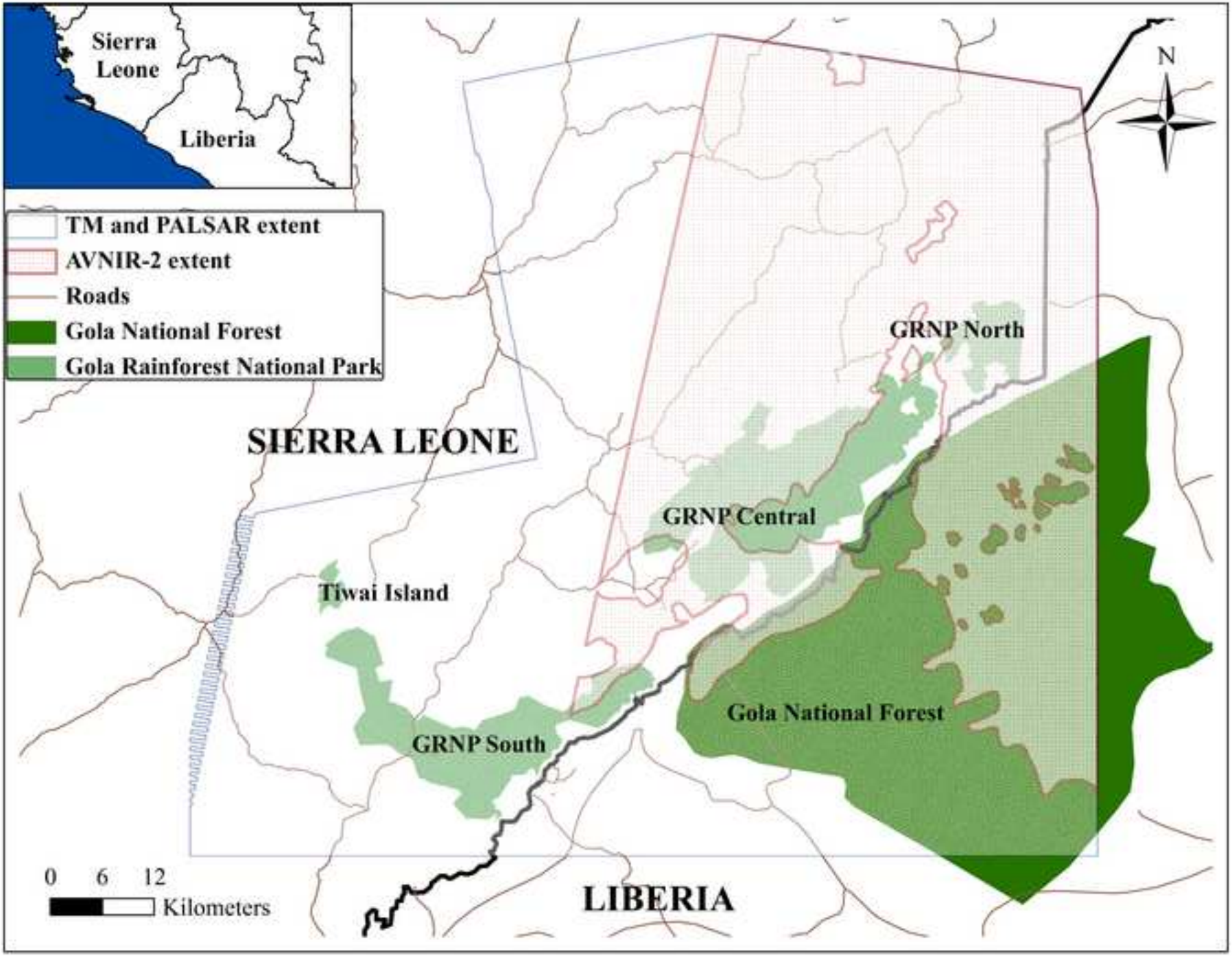

Figure

Click here to download high resolution image

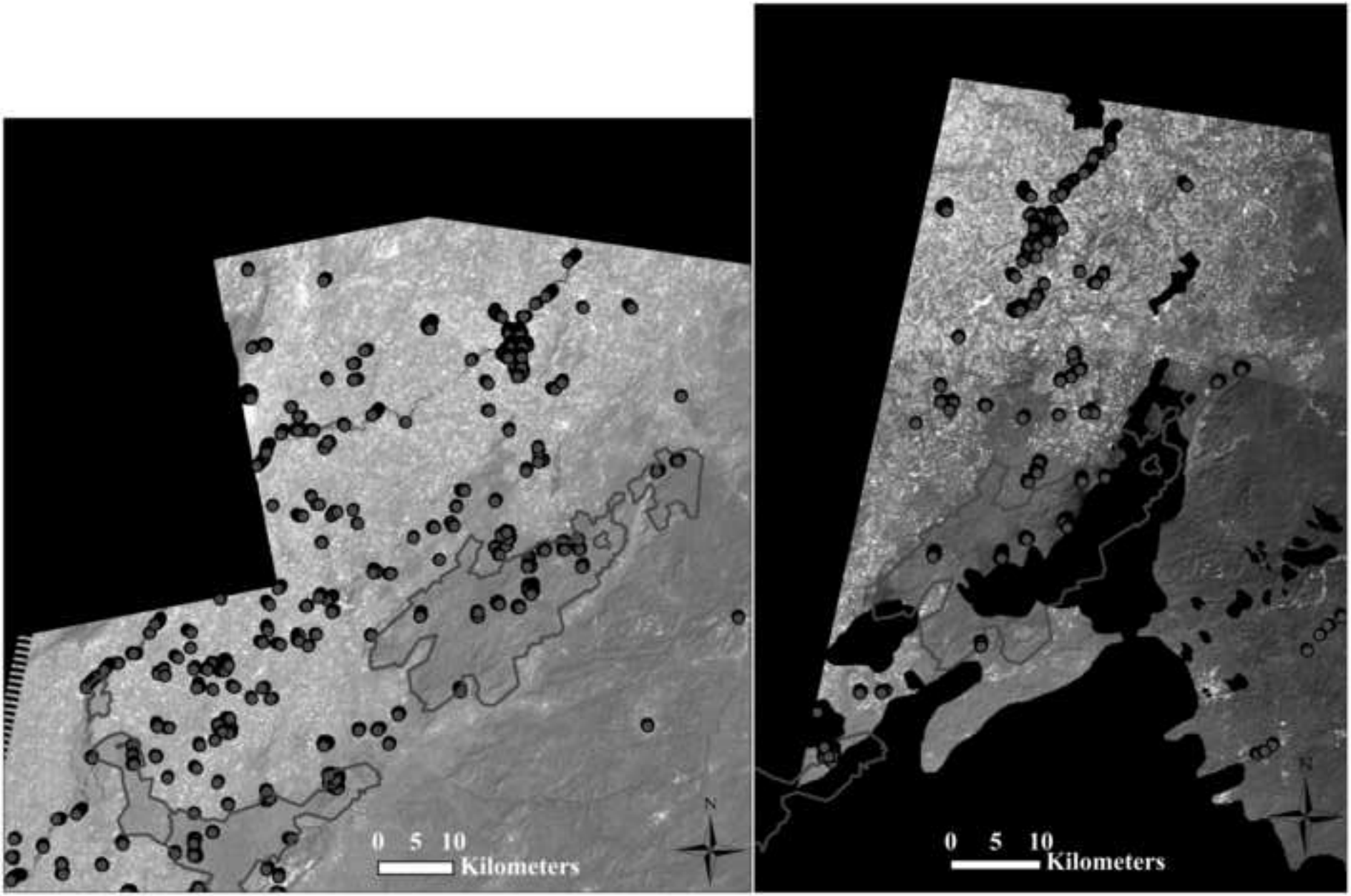

Figure

Click here to download high resolution image

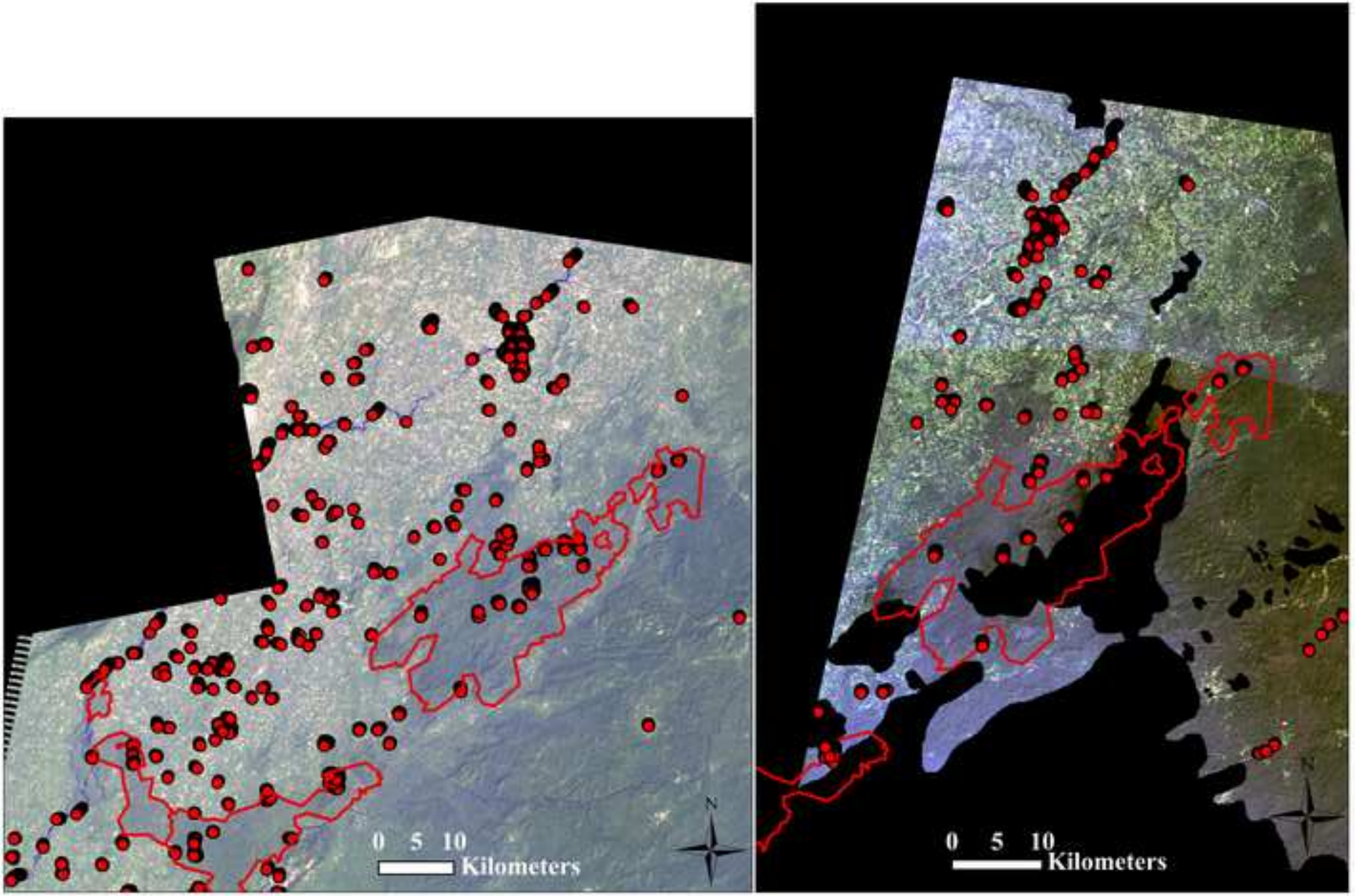

Figure

Click here to download high resolution image

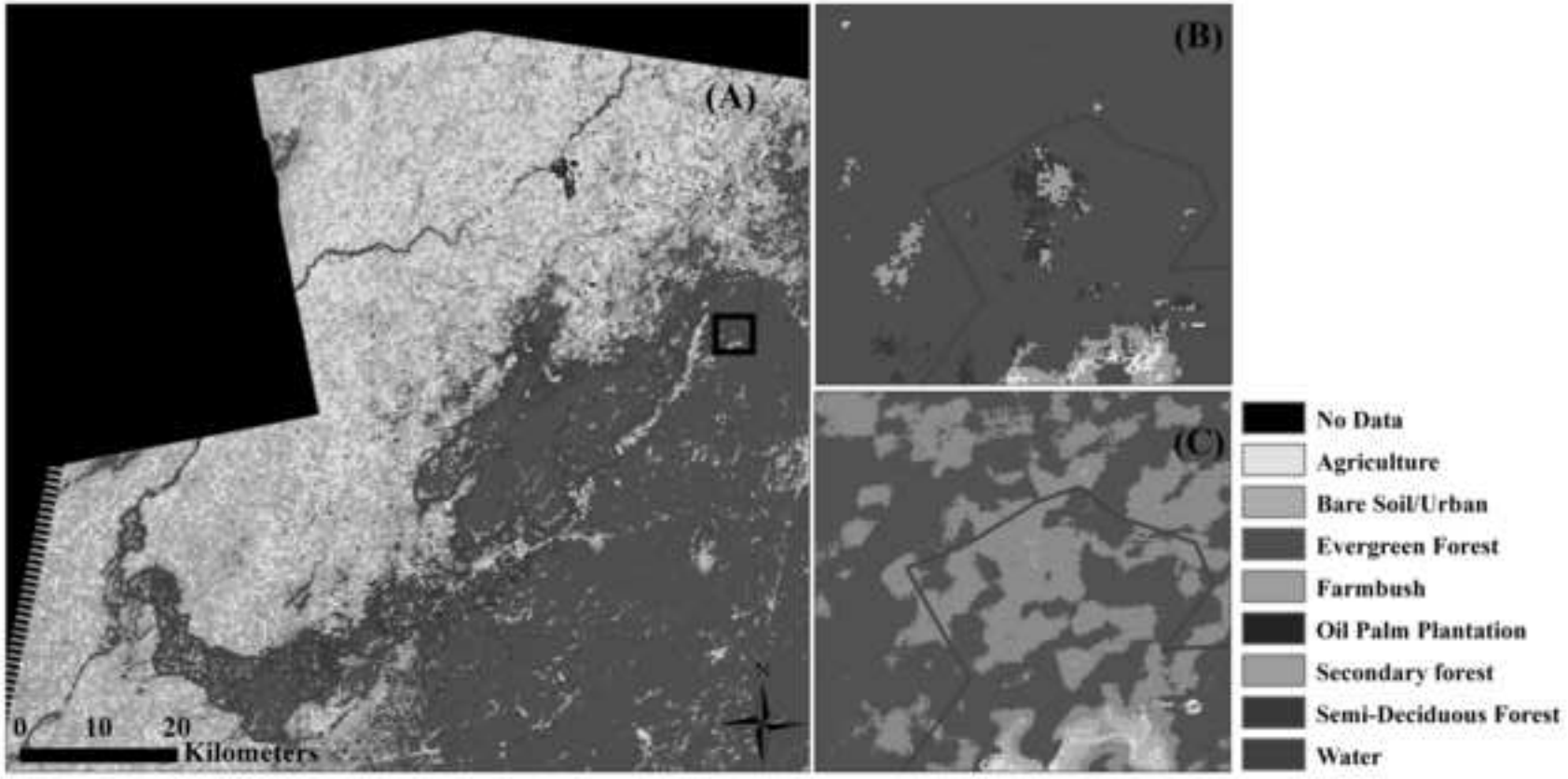

Figure

Click here to download high resolution image

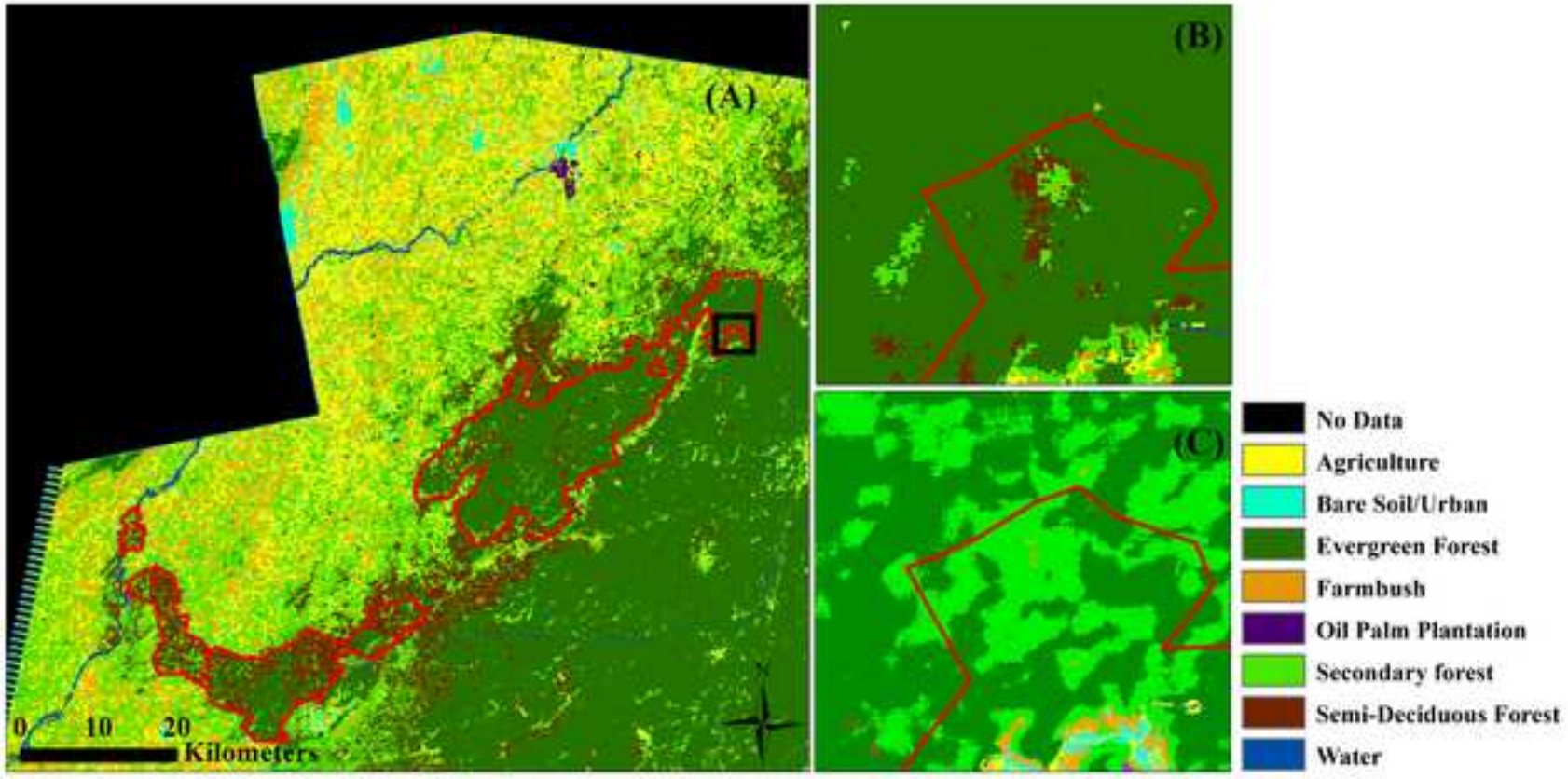

Figure

Click here to download high resolution image

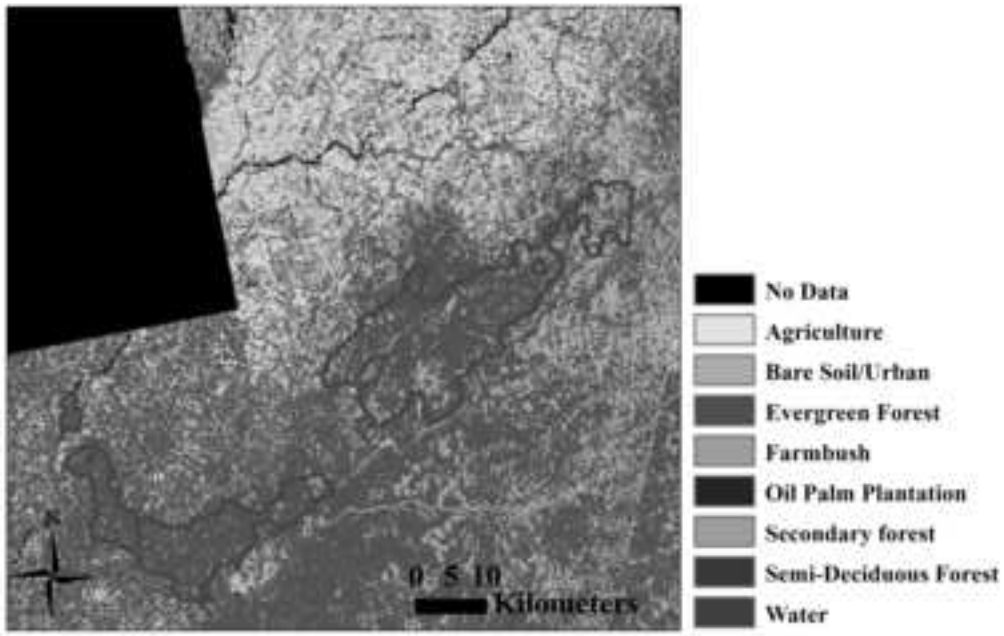

Figure

Click here to download high resolution image